Causal prefrontal contributions to stop-signal task performance in humans

Michael K. Yeung[1,2*#], Ami Tsuchida[3*], Lesley K. Fellows[1]

[1]Department of Neurology and Neurosurgery, Montreal Neurological Institute, McGill University, Quebec, Canada

[2]Department of Rehabilitation Sciences, The Hong Kong Polytechnic University, Hong Kong, China

[2]University of Bordeaux, GIN, IMN, UMR 5293, CEA, CNRS, Bordeaux, France

*Equal contributors

[#]Corresponding author:

Michael K. Yeung

kin-chung-michael.yeung@polyu.edu.hk

ST516, The Hong Kong Polytechnic University, Hong Kong, China

Abstract

The frontal lobes have long been implicated in inhibitory control, but a full understanding of the underlying mechanisms remains elusive. The stop-signal task has been widely used to probe instructed response inhibition in cognitive neuroscience. The processes involved have been modelled and related to putative brain substrates. However, there has been surprisingly little human lesion research using this task, with the few existing studies implicating different prefrontal regions. Here, we tested the effects of focal prefrontal damage on stop-signal task performance in a large sample of people with chronic focal damage affecting the frontal lobes (N=42) and demographically matched healthy people (N=60). Patients with damage to the left lateral, right lateral, dorsomedial, or ventromedial frontal lobe had slower stop-signal reaction time (SSRT) compared to healthy controls. There were systematic differences in the patterns of impairment across frontal sub-groups: those with damage to left or right lateral and dorsomedial frontal lobes, but not those with ventromedial frontal damage, were slower than controls to "go", as well as to stop. These findings suggest that multiple prefrontal regions make necessary but distinct contributions to stop-signal task performance. As a consequence, SSRT slowing is not strongly localizing within the frontal lobes.

Keywords: frontal lobe, lesion, inhibitory control, inferior frontal gyrus, impulsivity

Introduction

The ability to suppress inappropriate actions is key to flexible goal-directed behavior. Work in recent decades has defined component processes of response inhibition (assessed, for example, with go/no-go tasks and more recently with the stop-signal task) with increasing precision. The influential horse-race model conceives of this form of inhibitory control in terms of a race between the "go" response and a second, independent "stop" process (Logan & Cowan, 1984). The stop-signal task provides behavioral indicators of both processes, with the "go" reaction time (RT) measured directly on trials that do not require inhibition, and the stop-signal reaction time (SSRT) estimated by varying the delay between go and stop signals in the task (Lappin & Eriksen, 1966; Logan, 1994). This task and the associated computational framework have been widely applied in the study of neuropsychiatric conditions, many of which are characterized by impulsivity or other symptoms of weak inhibitory control (Alderson, Rapport, & Kofler, 2007; Lipszyc & Schachar, 2010; Smith, Mattick, Jamadar, & Iredale, 2014).

It is generally accepted that stop-signal-type response inhibition relies on fronto-striatal circuitry. It has been hypothesized that response inhibition is initiated by the frontal cortex, which activates the subthalamic nucleus and/or the striatum, exciting the globus pallidus pars interna and decreasing thalamocortical output (Aron & Poldrack, 2006; Nambu, Tokuno, & Takada, 2002). However, the evidence supporting this view is mixed, at least with respect to the role of specific frontal lobe subregions in humans. Meta-analyses of functional magnetic resonance imaging (fMRI) findings with the stop-signal task find more activity in successful-stop trials compared to go or failed-stop trials in several regions: left insula extending to thalamus and putamen, right insula extending to inferior frontal gyrus (IFG) and precentral gyrus, superior frontal gyrus

including the pre-supplementary motor area (pre-SMA) and premotor cortex, and right middle frontal gyrus (Rae, Hughes, Weaver, Anderson, & Rowe, 2014; Swick, Ashley, & Turken, 2011; Zhang, Geng, & Lee, 2017).

A somewhat different picture arises from loss of function experiments. There have been several studies using transcranial magnetic stimulation (TMS) to alter local cortical function. Notwithstanding the broad, bilateral frontal lobe activation observed in fMRI studies, this work has mainly focused on right IFG or dorsomedial PFC. Stimulation over the right IFG influenced SSRT in several (Chambers et al., 2006; Obeso, Cho et al., 2013; Obeso, Robles, Muñoz-Marrón, & Redolar-Ripoll, 2013; Verbruggen, Aron, Stevens, & Chambers, 2010), but not all (Lee et al., 2016) studies. TMS over the right pre-SMA can also affect SSRT (Obeso, Cho et al., 2013; Obeso, Robles et al., 2013), but this has not been a consistent finding (Lee et al., 2016; Verbruggen et al., 2010), and this region is challenging to reach with TMS. Several studies have found that TMS over the right middle frontal gyrus or primary motor cortex does not affect SSRT (Badry et al., 2009; Chambers et al., 2006; Obeso, Cho et al., 2013; Obeso, Robles et al., 2013; van den Wildenberg et al., 2010), supporting anatomical specificity within the frontal lobes.

Fixed focal lesions provide a second source of causal evidence, with more certainty about the anatomical extent of disruption than TMS. Studies of the effects of frontal lobe damage on response inhibition have yielded surprisingly mixed results. Early work reported that frontal lobe damage led to slower SSRT but did not address sub-regional contributions (Rieger et al., 2003). Donald Stuss and colleagues systematically studied sub-regional frontal lobe contributions to response inhibition in a relatively large sample, with the go/no-go task. They found that only the left superior medial frontal lobe made a necessary contribution (Picton et al., 2007). A second

study by Floden and Stuss (2006), this time with the stop-signal task, also supported a specific role for the dorsomedial frontal lobe: That paper reported that damage to the right superior frontal cortex led to slower SSRT. However, these findings are in contrast to another influential lesion study from about the same period showing that the extent of damage to the right IFG correlated with slower SSRT, and arguing for a specialized role of the right IFG in response stopping (Aron, Fletcher, Bullmore, Sahakian, & Robbins, 2003). Yet another study questioned the laterality of the IFG effect, finding that go/no-go task performance was impaired after left IFG damage (Swick, Ashley, & Turken, 2008). More recently, Roberts and Husain (2015) found intact stop-signal performance in a single case with a restricted pre-SMA lesion, raising questions about the dorsomedial frontal contribution to this task. However, this study used a stop signal procedure with equal probabilities of go and stop trials that might have encouraged strategic slowing and reduced reliability of the SSRT estimate (Verbruggen, Chambers, & Logan 2013).

This lack of consensus across human lesion studies, as well as uncertain convergence of lesion, TMS and fMRI findings poses problems for brain-based models of inhibitory control. This also raises doubts about applying the stop-signal task as a neuropsychological probe for specific fronto-striatal circuitry in neuropsychiatric conditions. Here, we aimed to provide causal evidence of regional frontal lobe contributions to the stop-signal task, studying a large sample of people with focal frontal lobe damage and age-matched healthy controls. To maximize applicability to the current cognitive neuroscience literature, we applied gold-standard recommendations for behavioral analysis (Verbruggen et al., 2019) and tested frontal lobe contributions with both region-of-interest and voxel-based approaches.

Methods

Participants

Forty-seven patients with focal damage to the frontal lobes were recruited via the research registries of the Center for Cognitive Neuroscience at the University of Pennsylvania and McGill University (Figure 1). Those with traumatic brain injury or other neurological conditions that might be associated with diffuse brain damage were excluded. All were administered the stop-signal task as part of a larger battery of tests. Forty-two patients met minimal performance criteria (described below) and were included in the current analysis. The group included 17 with ischemic or hemorrhagic stroke, 18 who had undergone resection of low-grade tumors, and 7 with damage due to ruptured aneurysm. Seventeen patients were taking one or more psychoactive medications, most commonly anticonvulsants or antidepressants. All patients were tested at least 6 months (range: 0.7 to 14.4 years) after the brain injury. The individual lesions of all frontal patients were manually traced from the most recent clinical magnetic resonance imaging or computed tomography imaging onto the standard Montreal Neurological Institute brain template by a neurologist blind to task performance, using MRIcro software (Rorden & Brett, 2000). In all cases, imaging was from at least six months post-event (typically more than 1-year post-event) i.e. reflecting the extent of chronic damage. Unfortunately, at this point, records of the imaging type were readily available for only the 23 patients imaged at McGill, 9 of which had CT, and 14 had 1.5T MRI. We are not making anatomical claims at a level of resolution that is likely to be affected by imaging modality.

Sixty-one age- and education-matched healthy participants were recruited via local advertisement in Montreal. None was taking psychoactive medication or reported a history of neurological or

psychiatric illness that might interfere with cognition. All control participants scored at least 26/30 (M = 27.8, SD = 1.3) on the Montreal Cognitive Assessment (MoCA; Nasreddine et al., 2005). One was excluded subsequently for failing to meet minimum performance criteria for the stop signal task (see Section 2.2.2), resulting in a final healthy control sample of 60 participants. All participants provided written informed consent, in accordance with the declaration of Helsinki. All were paid a nominal fee for their time. The study protocol was approved by the Institutional Review Boards of the University of Pennsylvania and McGill University.

Participants completed a brief battery of cognitive screening tests. Premorbid IQ was estimated using the American National Adult Reading Test (Blair & Spreen, 1989). Attention was assessed with the backward digit span and Corsi span tests, and executive function and language were assessed using the verbal fluency (phonemic (FAS) and semantic (animals)) and a sentence comprehension test similar to the token test (Lezak, 2004). Depression symptoms were assessed using the second edition of the Beck Depression Inventory (Beck, Steer, Ball, & Ranieri, 1996). All but two participants also completed a letter 2-back task involving a "go/no-go" decision requirement for a separate experiment: A fixed pseudorandom sequence of letters was presented at the center of the computer screen, one letter at a time. Participants were asked to respond by pressing the space bar as quickly as possible only when the letter they were seeing was identical to the letter they saw two trials before (i.e., target). They were asked to do nothing for all other letters (i.e., nontargets). On each trial, a letter was presented for 500 ms, followed by an interstimulus interval of 1500 ms. There was a total of 122 trials, 20 of which were target trials. A subset of the data from the 2-back task has been published previously (Tsuchida & Fellows, 2009). We included letter 2-back performance here as an ad hoc specificity check, considering it as a

control task of similar difficulty and with some requirements (e.g. sustained attention, motor response) that seem likely to be shared with the stop-signal task.

Stop-Signal Task

A version of the stop-signal task, similar to the one used in Aron et al. (2003) was administered. Each trial started with a blank screen for 1000 ms. Next, a left- or right-pointing arrow was presented in the center of the screen, and participants were instructed to respond with a left or right key press. The arrow stayed onscreen until a response was made. No time limit was set for responding. Stop signal trials were randomly interleaved, comprising 25% of the trials. On stop trials, participants heard an auditory tone (i.e., stop signal), in which case they were to withhold the response. Participants were instructed to respond to the arrows as quickly as possible and not to wait for the tone. The arrow stayed onscreen for a maximum of 1000 ms, disappearing when a response was made. The time between arrow presentation and stop signal (stop-signal delay (SSD)) was varied using four equiprobable staircases, starting at SSD values of 100, 200, 300, and 400 ms. The SSD for each staircase was decreased by 50 ms if a participant failed to inhibit a response and increased by 50 ms if the participant successfully inhibited the response. There were five blocks of 64 trials each, totaling 320 trials. During the break between blocks, the RT in the previous block was provided as feedback, and participants were reminded to respond as quickly as possible and not to wait for the tone. The task was presented using E-Prime 1.2 (Psychological Software Tools Inc., Pittsburgh, PA, USA).

In accordance with a recent consensus guide to stop-signal task analysis (Verbruggen et al., 2019), SSRT was estimated using the integration method. In this method, the point at which the stop process finishes is estimated by integrating the RT distribution and finding the point at which the

integral equals the probability of responding on stop signal trials. The finishing time of the stop process corresponds to the *n*th RT, where *n* refers to the number of RTs in the RT distribution of go trials multiplied by the overall probability of responding on stop signal trials. SSRT can then be estimated by subtracting the mean SSD from the *n*th RT. Go trials with a choice error were also included in SSRT estimation. The estimation of SSRT is unreliable if Stop RT is larger than go RT, or if the probability of inhibition on signal trials greatly differs from 50% (i.e., lower than 25% or higher than 75%). We excluded five participants, including one healthy control, two left lateral (LL) frontal patients, one dorsomedial (DM) frontal patient, and one bilateral lateral frontal patient, on the basis of these criteria. In addition, we excluded one ventromedial (VM) patient, who could not follow task instructions and achieved only 15% go trial accuracy.

Region of Interest Analysis

We divided the patients into four groups based on regions of interest implicated in the existing literature on response inhibition using the stop-signal (Rae et al., 2014; Swick et al., 2011; Zhang et al., 2017) or go/no-go tasks (Criaud & Boulinguez, 2013; Simmonds, Pekar, & Mostofsky, 2008; Swick et al., 2011). Patients were assigned to LL (N=6) or right lateral (RL; N=12) groups when damage involved the opercular and/or triangular parts of the IFG (BA 44, 45) in the left or right hemisphere. Patients were assigned to the DM group (N=13) when dorsomedial PFC, including the premotor cortex, SMA, or pre-SMA was the main site of damage. All other frontal patients were assigned to what we term the VM group (N=11): these patients had damage primarily affecting the ventromedial frontal cortex, orbitofrontal cortex (OFC), and/or pregenual anterior cingulate cortex and associated white matter, although the group was defined by the absence of damage to the hypothesized regions of interest rather than the presence of VM damage *per se*. We

used MRIcron software (Rorden, Karnath, & Bonilha, 2007) to estimate lesion volumes and generate overlap images (Figure 2). In addition, we examined whether the lesion sites of the patient groups overlapped with regions identified in the fMRI literature using the stop-signal task (Zhang et al., 2017). Figure 3 shows that all groups except the VM group had damage to regions that are consistently activated during successful stopping in the stop-signal task.

We conducted ANOVA and likelihood ratio tests to compare the demographic and neuropsychological test variables among groups. Post-hoc Tukey tests were carried out for pairwise comparisons. For the stop signal and letter 2-back test performance, initial analysis of data from healthy controls revealed significant effects of age on most of the stop-signal variables (mean go RT, $r_s = .63$, $p < .001$, mean failed-stop RT, $r_s = .64$, $p < .001$, go accuracy, $r_s = .37$, $p = .004$, mean SSD, $r_s = .60$, $p < .001$, and SSRT, $r_s = .51$, $p < .001$) and 2-back task variables (logistic equivalent discriminability measure d'_L, $r_s = -.31$, $p = .018$, and mean correct hit RT, $r_s = .30$, $p = .020$). Because age is also associated with more variable cognitive task performance (Christensen et al., 1999), we applied the age adjustment method proposed by Altman (1993), which considers not only the age-specific mean but also the age-specific standard deviation (*SD*) of outcome measures. This approach minimized confounding from age in the performance-based analyses, enabling a more accurate estimation of lesion effects. Accordingly, we generated age-adjusted *z*-scores for all variables, and used these as the primary variables of interest. However, we provide the raw performance variables in each group in order to facilitate comparisons with the existing literature.

To generate the age-adjusted *z*-scores (Altman, 1993), a variable of interest (e.g. SSRT) was first regressed by age to obtain the predicted values for that variable at different ages. Next, the age-

specific *SD* was estimated by regressing the absolute values of the residual on age, then multiplying the predicted values of the absolute residuals by $(\pi/2)^{0.5}$. Finally, the age-adjusted *z*-score was computed by subtracting the predicted from the observed value of the variable at a given age, then dividing it by the estimated age-specific *SD*. We used the data from the HC group to derive the age-specific *SD*, and computed the age-adjusted SSRT for each participant.

In addition, Shapiro–Wilk tests revealed a violation of the normality assumption for some performance variables (*p*s < .05) In healthy controls, Shapiro–Wilk tests revealed non-normal distributions for the age-adjusted *z*-scores for SSRT, $p = .025$, mean go RT, $p = .031$, mean failed stop RT, $p = .029$, and go accuracy, $p < .001$, on the stop-signal task, and for mean hit RT on the 2-back task, $p < .001$. In patients, the age-adjusted *z*-scores for some stop-signal task variables were not normally distributed (LL: mean go RT, $p = .021$; RL: SSRT, $p = .001$, and mean go RT, $p = .021$; VM: go accuracy, $p = .001$). There was an extreme outlier in the RL group, but this outlier was not removed because this individual met the criteria for SSRT estimation and was 97% accurate on the stop-signal task.

Since some of these variables were still not normally distributed after log-transformation (e.g., the age-adjusted *z*-scores for SSRT in the RL group), and the sample sizes of the region-of-interest groups were not large, we used nonparametric Kruskal–Wallis tests to compare performance among groups. Significant group effects were followed up with *post-hoc* one-tailed Mann–Whitney *U* tests for pairwise group comparisons (each frontal group vs. healthy controls) to test the directional hypothesis that performance in those with frontal damage was worse than healthy controls. Significance level for these *post-hoc* tests was Bonferroni corrected (i.e. to $p < 0.013$) for the four group comparisons. The significance level was set at 0.05 for all other statistical tests,

unless otherwise specified. We also report the effect size *r*, calculated as $z/\sqrt{N}$, where the *z*-value is approximated from the *U* test statistics, and *N* represents the sample size (Fritz, Morris, & Richler, 2011). All analyses were performed using SPSS 23.0 (IBM Inc., Armonk, NY, USA).

Lesion-Symptom Mapping

We followed up the region-of-interest analysis with voxel-based lesion-symptom mapping (VLSM; Rorden et al., 2007) and support vector regression lesion-symptom mapping (SVR-LSM; Zhang, Kimberg, Coslett, Schwartz, & Wang, 2014) to identify the clusters of damage within the frontal lobes that contributed to impaired stop-signal performance. The performance measure of interest (i.e., age-adjusted *z*-score for SSRT) was entered as a continuous variable.

For the VLSM analysis, statistical comparisons were made for each eligible voxel, comparing the performance of patients with a lesion affecting a given voxel to that of patients with a lesion sparing that voxel. We used the nonparametric Brunner–Munzel test to perform statistical comparisons on a voxel-wise basis (Brunner & Munzel, 2000), as implemented in the open-source NPM and MRIcron software (Rorden et al., 2007). In this analysis, only voxels affected in at least three cases (i.e., ≥ 5% of the whole sample) were included (Sperber & Karnath, 2017). Clusters with at least 50 voxels yielding a *Z* score greater than 1.65 (uncorrected $p < 0.05$) are reported. We used the Brunner–Munzel test because the age-adjusted *z*-scores for SSRT among the 42 patients were not normally distributed (Shapiro–Wilk test: $p < .001$), rendering the use of parametric tests inappropriate. While Spearman's correlation showed no significant correlation between lesion volume and the age-adjusted *z*-scores for SSRT among patients, $r_s = .17$, $p = .29$, we performed the VLSM analysis after regressing lesion volume out of the age-adjusted *z*-scores for SSRT to remove error variance related to lesion size.

The SVR-LSM was performed using the SVR-LSMtbx (Zhang et al., 2014). This method uses all lesion voxels as input and finds a behavior predictive model; the trained model's predictive hyperplane is then back projected into the data space, which can be overlaid on a brain template for interpretation. In accordance with the findings and recommendations of previous studies (DeMarco & Turkeltaub, 2018; Wiesen, Sperber, Yourganov, Rorden, & Karnath, 2019; Zhang et al., 2014), the cost parameter C and the parameter γ were set at 30 and 5, respectively. Only voxels damaged in at least three patients were selected. Lesion size was controlled for using direct total lesion volume control (Zhang et al., 2014). The SVR-β map was thresholded using false discovery rate correction (q = .05) and cluster size correction (≥ 50 voxels).

Results

Demographic and Neuropsychological Characteristics

Demographic information and screening neuropsychological test results are provided in Table 1. There were no significant differences in age, gender, or education between frontal patients and healthy controls, ps > .11. Among patients, there were no significant differences in lesion volume, p = .18, or time after brain injury, p = .94.

Stop-Signal Task Performance

Table 2 presents the stop-signal task performance of all participants who met the performance criteria for the task. All participants (except one VM patient excluded from analysis) performed the go trials at ≥ 85% accuracy. A Kruskal–Wallis test revealed no significant difference in the age-adjusted z-scores for go accuracy among groups, p = .22.

Figure 4 presents the SSRT of each group. Kruskal–Wallis tests revealed a significant difference in the age-adjusted *z*-scores for SSRT among groups, χ^2 = 14.22, p = .007. Post-hoc Mann–Whitney *U* tests showed that the LL group had significantly slower SSRT than healthy controls (p = .002, r = .35). Although not reaching the Bonferroni-corrected threshold of $p < 0.013$, all frontal groups had a tendency for slower SSRT than healthy controls (RL, p = .034, r = .22; DM, p = .018, r = .24; VM, p = .043, r = .20). Thus, while only the LL group differed significantly from the healthy control as a group, damage to any of the pre-defined prefrontal sub-regions tended to be associated with slower SSRT, with medium effect sizes in all groups.

All the results were identical when the SSRT of each participant was re-estimated by substituting all RTs slower than 2000 ms with this maximal response latency (Verbruggen et al., 2013); the number of RTs slower than 2000 ms did not significantly differ among groups (Kruskal–Wallis test: p = .058). We also checked the robustness of the SSRT results by substituting parametric tests after removing an extreme outlier value in the RL group and replacing it with the next most extreme value in the same group. Effects were very similar to those reported. To test for finer-grained structure-function relationships, including any that might cross pre-specified region-of-interest boundaries, the relationship between SSRT and lesion location was also tested using VLSM and SVR-LSM. As can be seen from the power map in Figure 5, the sample had sufficient statistical power (i.e., voxels damaged in at least 3 people) to detect effects in most parts of the medial wall of the frontal cortex, bilateral inferior frontal gyri, and right middle frontal gyrus.

None of the voxels in the VLSM analysis using the Brunner–Munzel tests survived correction for multiple comparisons. However, uncorrected results revealed damage to the left IFG and insula (X = -43, Y = 25, Z = 6; BA 13/45), right insula (MNI coordinates: X = 40, Y = 8, Z = 14; BA

13), and left presupplementary motor area (X = -7, Y = 37, Z = 48; BA 8) as most strongly linked with slower SSRT (Figure 5). Medina et al. (2010) argued that the Brunner–Munzel test would yield large Type I errors if the sample size of either lesion or the control group was less than 10, and suggested the use of a more conservative permutation-derived correction when using these tests in the context of small samples. In the present study, no voxels survived any kind of multiple comparison correction even before the permutation-derived correction, and we report uncorrected voxels with $Z > 1.65$ only to illustrate brain regions most associated with SSRT. Thus, our interpretation of the VLSM results would not change after considering the sample size requirement of the Brunner–Munzel test.

As for the SVR-LSM analysis, no voxels survived correction, therefore we report the SVR-β map showing the top 5% voxels with the highest β values (i.e., most predictive of SSRT) for illustration purposes. Similar to VLSM, SVR-LSM identified damage to the bilateral IFG/insula and subregions within the dorsomedial frontal cortex (X = 1, Y = 12, Z = 66; BA 6; bilateral supplementary motor area (SMA) but not left pre-SMA) to be most strongly associated with slower SSRT. Unlike VLSM, it identified damage to the right frontopolar and orbitofrontal cortex (X = 10, Y = 57, Z = -6; BA 10/11) as most strongly linked with slower SSRT, in keeping with the region-of-interest analysis.

An early study by Aron et al. (2003) found positive correlations between SSRT and lesion volume in both the right BA44 (r = .57) and BA45 (r = .65). In an effort to replicate this observation, we calculated one-tailed Spearman's correlations to assess the relationships between the raw SSRT and lesion volume in these two Brodmann areas. No significant correlation was found for BA 44, r_s = -.08, p = .31, BA 45, r_s = .00, p = .49, or BA 44 and BA 45 combined, r_s = .11, p = .47.

Differential Contributions of Prefrontal Regions to Response Stopping

Because the estimation of SSRT depended on the probability of inhibiting a response, mean SSD, and go RT, we next asked which of these variables drove the slower SSRT in the frontal patients. Kruskal–Wallis tests revealed no significant group differences in the age-adjusted *z*-scores for the probability of inhibiting a response or for mean SSD, *p*s > .26. However, we found a significant difference in the age-adjusted *z*-scores for mean go RT, χ^2 = 14.57, p = .006. Post-hoc Mann–Whitney *U* test with an adjusted *p*-value of 0.013 revealed that both the LL, p = .003, r = .33, and DM, p =.007, r = .29, groups had significantly slower go RT than healthy controls (Figure 6a). At the uncorrected *p*-value threshold of 0.05, RL group also had slower go RT, p = .021, r = .24, while the VM group was indistinguishable from controls, p = .49, r = .00.

Further analysis revealed that this response slowing was not specific to go trials, because there was also a significant group difference in the age-adjusted *z*-scores for mean RT on failed stop-signal trials, χ^2 = 17.33, p = .001, which was again driven by significantly slower failed-stop RT in the LL group, p = .003, r = .33, and DM group, p = .004, r = .31, compared to healthy controls (Figure 6b). Failed-stop RT in the RL group was also significantly slower than in healthy controls, p = .011, r = .27. In contrast, the VM group was as fast to respond as healthy controls, p = .35, r = .05. The effect sizes for both the go RT and failed-stop RT were medium for the DM, LL, and RL groups, while they were very small for the VM group. Thus, the LL and DM groups, and the RL group to a lesser extent, were all slower than healthy controls to go, regardless of trial type.

Despite instructions and feedback that emphasized rapid responses, it is possible that the slow RT in the frontal groups was attributable to strategic slowing (i.e. “waiting” for the stop signal). We compared the mean raw go RT across the four blocks of the task to evaluate whether slowing

occurred over the task, within each group. Friedman tests revealed no significant differences in mean go RT across blocks in any group, although there was a statistical trend for the effect of block in the LL group, $\chi^2 = 6.60$, $p = .086$ (all other groups: ps > .14). Thus, go RT was relatively stable over time throughout the task at the group level, with the exception of the LL group tending to slow down across blocks. We also examined slowing at the individual level by analyzing the slope of a regression line fit to mean go RT across the four blocks. A Friedman test revealed no significant differences in the slope among the five groups, $\chi^2(4) = 5.62$, $p = .23$, but there was large variability in this slope among patients. For the 42 patients, Spearman's correlation (two-tailed) revealed no significant correlation between the slope of mean go RT and the age-adjusted z-score for SSRT, $r_s = .23$, $p = .15$, suggesting a weak, if any, relationship between slowing across blocks and SSRT among frontal patients.

One study has found that the SSRT estimated by the block-based integration method was more accurate than that estimated using the experiment-wise integration method when participants exhibit slowing over time (Verbruggen, Chambers, & Logan, 2013). To check the robustness of our results, we repeated the analyses with the block-based method: SSRT was estimated for each block separately before averaging the four estimates. The block-based integration method yielded results similar to the experiment-wise integration method. That is, a Kruskal–Wallis test revealed a significant difference in the age-adjusted z-scores for SSRT among groups, $\chi^2(4) = 16.82$, $p = .002$. Post-hoc Mann–Whitney U tests showed that the LL group, $p = .005$, $r = .32$, RL group, $p = .004$, $r = .31$, and DM group, $p = .008$, $r = .28$, had significantly slower SSRT than healthy controls. At the uncorrected p-value threshold of 0.05, the VM group also had slower SSRT, $p = .019$, $r = .25$. These results indicate that the finding of slower SSRT following damage to any prefrontal region is robust across estimation methods.

Specificity

The finding that damage to any of the pre-specified prefrontal regions was associated with slower response stopping could be explained by a more generic deficit due to brain damage or illness, such as psychomotor slowing, inattention or low motivation. To address the specificity of the stop-signal task observations, we took advantage of a second dataset available in the same sample (missing data for two frontal patients) to compare performance on a letter 2-back task that involved a "go/no-go" response requirement (i.e. button press to targets, no response to non-targets). Mann–Whitney *U* tests conducted on the age-adjusted z-scores for d'_L and hit RT with an adjusted *p*-value of 0.013 showed that only the DM group had a significantly lower d'_L (*M* = -0.73, *SD* = 0.74), *p* = .008, *r* = .28, and slower hit RT (*M* = 0.78, *SD* = 0.92), *p* = .003, *r* = .33, than healthy controls. At the uncorrected *p*-value threshold of 0.05, the LL group also had a lower d'_L (*M* = -0.70, *SD* = 1.11), *p* = .040, *r* = .22, and slower RT (*M* = 0.88, *SD* = 1.03), *p* = .029, *r* = .24, than healthy controls. By contrast, the d'_L and hit RT of both RL group (d'_L: *M* = 0.08, *SD* = 1.13; RT: *M* = 0.19, *SD* = 1.30) and VM group (d'_L: *M* = -0.59, *SD* = 1.44; RT: *M* = -0.22, *SD* = 0.79) were comparable to those of healthy controls, *p*s > .15, *r*s < .12. Regardless of the measure, the effect sizes were medium for the DM and LL groups, and the effect sizes were small or very small for the RL and VM groups.

The DM and LL groups exhibited impairment in both tasks, whereas the RL and VM groups exhibited impairment only in the stop-signal task. To directly explore whether there was a dissociation between the stop-signal and 2-back task performance in RL and VM patients but not in DM and LL patients, we performed two separate mixed ANOVA with group (HC and DM/LL; HC and RL/VM) as between-subjects factor and task (SSRT, d'_L) as within-subjects factor on the

age-adjusted *z*-scores (the age-adjusted *z*-score for d'_L was reversed such that a higher score represented poor performance). Groups that exhibited a similar pattern were combined to increase power; the results must be taken with caution given that this analysis is post hoc. For the ANOVA with the RL/VM group, the main effect of group was significant, $F(1, 81) = 7.11$, $p = .009$, $\eta_p^2 = .081$. More importantly, the interaction between group and task was also marginally significant, $F(1, 81) = 3.71$, $p = .058$, $\eta_p^2 = .044$. For the ANOVA with the DM/LL group, the main effect of group was significant, $F(1, 75) = 17.09$, $p < .001$, $\eta_p^2 = .19$, but the interaction between group and task was not, $F(1, 75) = 0.82$, $p = .37$, $\eta_p^2 = .01$. These results suggest the possibility of a dissociation between stop-signal and 2-back task performance in RL/VM patients only.

Discussion

This study examined the effects of focal frontal lobe damage on the widely used two-choice stop-signal task, aiming to provide causal evidence for the regional prefrontal contributions to response stopping. We failed to find strong evidence for a localized effect of damage to a specific prefrontal region. Rather, we found that damage to any of the prefrontal regions tended to prolong SSRT compared to healthy controls. The VLSM and SVR-LSM analyses confirmed diffuse effects of frontal damage on SSRT. The uncorrected z-score and SVR-β maps indicated that bilateral IFG and underlying white matter, extending to the insula, as well as dorsomedial frontal cortex, were most associated with slower SSRT.

These findings provide converging support for the extensive functional neuroimaging literature on this task. Several recent fMRI meta-analyses have shown activation in bilateral IFG and superior frontal cortex during successful response stopping (Rae et al., 2014; Swick et al., 2011; Zhang et al., 2017). While our study focused on frontal lobe damage, we also observed effects of damage

in the anterior insula bilaterally, in keeping with the fMRI literature. However, damage to the IFG and insula typically co-occur, given their shared vascular supply, so this observation in this sample should be interpreted with caution. A study including patients with insula lesions sparing the IFG is needed to strongly test the independent contribution of the insula to stop-signal task performance.

We took advantage of pre-existing data on a letter 2-back task with some demands in common with the stop-signal task to provide evidence that the rather diffuse effect of frontal damage observed on the stop-signal task was not merely a nonspecific consequence of brain damage. While RL and VM patients had increased SSRT on the stop-signal task, they were not particularly slow or inaccurate on the 2-back task. These findings suggest that the impaired stop-signal task performance in these patients cannot be readily explained by generic factors such as inattention, non-specific response slowing or low motivation. Instead, it seems likely that multiple prefrontal regions, their interconnections, and their connections with striatal systems are required for stop-signal task performance, such that focal damage in many frontal lobe areas can yield impairment. However, this study was not designed to assess potential contributions from posterior brain regions. Given the unexpectedly diffuse effect of damage to any of the frontal regions-of-interest on stop-signal task performance, we cannot entirely exclude that the observed impairment in all patient groups may be due to brain damage in general.

Previous efforts to demonstrate a critical role for frontal lobe subregions in response inhibition have provided mixed results. Some of this variability is inherent to lesion studies, which often involve small samples with heterogeneous coverage of key cortical regions and white matter tracts. There are also potentially important differences in the parameters of the behavioral tasks used

across studies. Here we recruited a large sample, with power to test several regions implicated in the task by individual lesion studies, TMS research, and fMRI findings. Aiming for replication, we used task parameters that were very similar to those in Aron et al (2003). We also adopted recent consensus guidelines for behavioral analysis (Verbruggen et al., 2019), minimizing the risk of 'cherry-picking' with respect to the behavioral data. While our findings corroborate those reported by Aron et al. (2003) that damage to the right IFG prolongs SSRT, the strong specificity claim put forward in that study is not supported. Instead, we also find evidence for contributions of left IFG and bilateral dorsomedial frontal lobe (likely pre-SMA specifically, with left hemisphere damage more strongly linked to impairment than right). These additional regions have been implicated in prior lesion studies. A critical role for dorsomedial frontal cortex was noted by Floden and Stuss (2006), although not confirmed by a single case study of a patient with right pre-SMA damage, albeit with stop-signal task parameters that differed from those used in the other studies (Roberts & Husain, 2015). Swick et al. (2008) also reported increased false alarms on the go/no-go task in 12 patients who had a maximal lesion overlap in the left posterior IFG.

Given that previous studies using the stop-signal (Aron et al., 2003; Floden & Stuss, 2006) and go/no-go tasks in patients with frontal damage (Picton et al., 2007; Swick et al., 2008) have not implicated the ventromedial frontal lobe, our finding of SSRT slowing in the VM group, albeit only at an uncorrected threshold, was unexpected. Of note, the Swick et al. (2008) study shows maximal lesion overlap in the OFC group in the anterior OFC, whereas the group we studied had maximal damage to the posterior OFC extending into subcortical structures and adjacent insula while, by design, sparing the IFG. Lesion-symptom mapping inconsistently identified the contribution of OFC sub-regions to SSRT at an uncorrected threshold. Thus, we speculate that the observed effects in the 'VM' group may be related to disruption of white matter connections

between the inferior frontal lobe and subcortical regions, circuits which have been hypothesized to underlie response inhibition, or motor control in general (Aron & Poldrack, 2006; Nambu et al., 2002), rather than to damage to orbitofrontal or ventromedial prefrontal cortex. Further work will be needed to address this possibility, perhaps by systematically characterizing the distant as well as local impact of focal lesions (Nomura et al., 2010, Foulon et al 2018).

In agreement with some previous findings (Aron et al., 2003; Rieger et al., 2003), frontal patients overall were found to have slower go RT, with the notable exception of the VM group. In contrast, Floden and Stuss (2006) reported intact go RT in frontal patients, but unlike other studies and the present study, Floden and Stuss used a different two-choice RT task involving letter stimuli and a fixed SSD. The discrepancy in findings with respect to response speed may thus be due to different task characteristics. In the present study, DM and LL frontal patients were found to be slower to respond on both the stop-signal and 2-back tasks. Thus, the slowed responses in the stop-signal task might be attributable to general response slowing in those groups. In contrast, RL patients were slow to go on the stop-signal but not the 2-back task, suggesting disruption of a "go" process specific to the stop-signal task. While we instructed the participants to respond as quickly as possible, RL patients might have strategically slowed their responses to increase the likelihood of successful response suppression, i.e. to compensate for impaired stopping. Future work would benefit from including a baseline block without stop signal trials to better characterize strategic slowing, if any.

It is not clear why the mean go RTs reported in the present study were more than 100 ms longer than those reported in Aron et al. (2003) despite highly similar stop-signal procedures. The two study samples had comparable demographics. Aron et al. (2003) did not report the probability of

stopping on stop signal trials, but it was stated that convergence to a 50% suppression rate was ensured, and that mean SSD was computed after convergence on this suppression rate. In the present study, all groups had a mean suppression rate greater than 50% (e.g., HC: 57%). Thus, the slower go RTs may be due to more slowing among our participants, although they nonetheless meet currently recommended performance criteria for SSRT estimation.

The present findings of the diffuse effect of frontal lesions on stop-signal task performance may reflect the complexity of this task. Despite its conceptual elegance, the stop-signal task engages multiple component processes, including the establishment of stimulus-response relationships, response selection, stop signal detection, behavioral adjustment, and monitoring of responses over time. Previous studies have implicated the dorsomedial frontal cortex in selection of appropriate responses (Mostofsky & Simmonds, 2008) and rapid, within-trial response adjustment (Modirrousta & Fellows, 2008), the left lateral frontal cortex in task setting (Stuss & Alexander, 2007), and the right (inferior) frontal cortex in monitoring (Stuss & Alexander, 2007) and implementing a brake over response tendencies (Aron, Robbins, & Poldrack, 2014). Thus, stop-signal task performance can be conceived of as the product of several component processes, each of which draws critically on different parts of the frontal lobe. Accordingly, impaired SSRT can reflect impairment in any one or more of these processes, each potentially related to disruption of specific regional frontal lobe damage or associated circuits.

Stuss et al. suggested a different framework, proposing that the frontal sub-regional contributions to inhibitory control involved energization, task setting, and monitoring processes (Stuss & Alexander, 2007). The stop-signal task would presumably draw, at least to some degree, on all of

these. The present results are broadly compatible with this alternate framework, although our study was not designed to test it.

In summary, our findings demonstrate that multiple subregions within the PFC are necessary for performance of the stop-signal task. While slowed SSRT (i.e., impaired stop process) can reflect dysfunction of any prefrontal region, the pattern of both slowed go RT and slowed SSRT was observed after damage to left or right lateral or dorsomedial frontal regions. This reconciles much of the existing lesion literature, which has found evidence for a role for each of these regions individually. These findings suggest caution in interpreting the frontal lobe basis of observed impairments of stop-signal task performance in neuropsychiatric conditions such as attention-deficit/hyperactivity disorder or obsessive-compulsive disorder (Alderson, Rapport, & Kofler, 2007; Lipszyc & Schachar, 2010). Likewise, the stop-signal task may be a useful probe of frontal function in neurological conditions but cannot be used to support finer-grained sub-regional localization within the frontal lobes.

Conflict of Interest Statement

The authors have no conflicts of interest to declare.

Acknowledgements

We thank the database managers at the University of Pennsylvania (Marianna Stark) and the McGill Cognitive Neuroscience Research Registry (Arlene Berg), and clinical colleagues at both sites for their help with patient recruitment. Appreciation is also extended to the volunteers who made this research possible through their generous participation. This work was supported by the

Canadian Institutes of Health Research and a Canada First Research Excellence Fund grant to McGill University (Healthy Brains for Healthy Lives).

References

Alderson, R. M., Rapport, M. D., & Kofler, M. J. (2007). Attention-deficit/hyperactivity disorder and behavioral inhibition: a meta-analytic review of the stop-signal paradigm. *Journal of abnormal child psychology, 35*(5), 745-758.

Altman, D. G. (1993). Construction of age-related reference centiles using absolute residuals. *Statistics in medicine, 12*(10), 917-924.

Aron, A. R., & Poldrack, R. A. (2006). Cortical and subcortical contributions to stop signal response inhibition: role of the subthalamic nucleus. *Journal of Neuroscience, 26*(9), 2424-2433.

Aron, A. R., Fletcher, P. C., Bullmore, E. T., Sahakian, B. J., & Robbins, T. W. (2003). Stop-signal inhibition disrupted by damage to right inferior frontal gyrus in humans. *Nature neuroscience, 6*(2), 115-116.

Aron, A. R., Robbins, T. W., & Poldrack, R. A. (2014). Inhibition and the right inferior frontal cortex: one decade on. *Trends in cognitive sciences, 18*(4), 177-185.

Badry, R., Mima, T., Aso, T., Nakatsuka, M., Abe, M., Fathi, D., ... & Fukuyama, H. (2009). Suppression of human cortico-motoneuronal excitability during the Stop-signal task. *Clinical Neurophysiology*, *120*(9), 1717-1723.

Beck, A. T., Steer, R. A., Ball, R., & Ranieri, W. F. (1996). Comparison of Beck Depression Inventories-IA and-II in psychiatric outpatients. *Journal of personality assessment*, *67*(3), 588-597.

Blair, J. R., & Spreen, O. (1989). Predicting premorbid IQ: a revision of the National Adult Reading Test. *The Clinical Neuropsychologist*, *3*(2), 129-136.

Brunner, E., & Munzel, U. (2000). The nonparametric Behrens-Fisher problem: Asymptotic theory and a small-sample approximation. *Biometrical Journal: Journal of Mathematical Methods in Biosciences*, *42*(1), 17-25.

Chambers, C. D., Bellgrove, M. A., Stokes, M. G., Henderson, T. R., Garavan, H., Robertson, I. H., ... & Mattingley, J. B. (2006). Executive "brake failure" following deactivation of human frontal lobe. *Journal of cognitive neuroscience*, *18*(3), 444-455.

Christensen, H., Mackinnon, A. J., Korten, A. E., Jorm, A. F., Henderson, A. S., Jacomb, P., & Rodgers, B. (1999). An analysis of diversity in the cognitive performance of elderly community dwellers: individual differences in change scores as a function of age. *Psychology and aging*, *14*(3), 365-379.

Criaud, M., & Boulinguez, P. (2013). Have we been asking the right questions when assessing response inhibition in go/no-go tasks with fMRI? A meta-analysis and critical review. *Neuroscience & biobehavioral reviews*, *37*(1), 11-23.

DeMarco, A. T., & Turkeltaub, P. E. (2018). A multivariate lesion symptom mapping toolbox and examination of lesion-volume biases and correction methods in lesion-symptom mapping. *Human brain mapping*, *39*(11), 4169-4182.

Floden, D., & Stuss, D. T. (2006). Inhibitory control is slowed in patients with right superior medial frontal damage. *Journal of cognitive neuroscience*, *18*(11), 1843-1849.

Foulon, C., Cerliani, L., Kinkingnehun, S., Levy, R., Rosso, C., Urbanski, M., ... & Thiebaut de Schotten, M. (2018). Advanced lesion symptom mapping analyses and implementation as BCBtoolkit. *GigaScience*, *7*(3), giy004.

Fritz, C. O., Morris, P. E., & Richler, J. J. (2012). Effect size estimates: current use, calculations, and interpretation. *Journal of experimental psychology: General*, *141*(1), 2.

Lappin, J. S., & Eriksen, C. W. (1966). Use of a delayed signal to stop a visual reaction-time response. *Journal of Experimental Psychology*, *72*(6), 805-811.

Lee, H. W., Lu, M. S., Chen, C. Y., Muggleton, N. G., Hsu, T. Y., & Juan, C. H. (2016). Roles of the pre-SMA and rIFG in conditional stopping revealed by transcranial magnetic stimulation. *Behavioural brain research*, *296*, 459-467.

Lezak, M. D., Howieson, D. B., Loring, D. W., & Fischer, J. S. (2004). *Neuropsychological assessment*. Oxford University Press, USA.

Lipszyc, J., & Schachar, R. (2010). Inhibitory control and psychopathology: a meta-analysis of studies using the stop signal task. *Journal of the International Neuropsychological Society*, *16*(6), 1064-1076.

Logan, G. D. (1994). *On the ability to inhibit thought and action: A users' guide to the stop signal paradigm.* In D. Dagenbach & T. H. Carr (Eds.), *Inhibitory processes in attention, memory, and language* (p. 189–239). Academic Press.

Logan, G. D., & Cowan, W. B. (1984). On the ability to inhibit thought and action: A theory of an act of control. *Psychological review*, *91*(3), 295-327.

Medina, J., Kimberg, D. Y., Chatterjee, A., & Coslett, H. B. (2010). Inappropriate usage of the Brunner–Munzel test in recent voxel-based lesion-symptom mapping studies. *Neuropsychologia*, *48*(1), 341-343.

Modirrousta, M., & Fellows, L. K. (2008). Dorsal medial prefrontal cortex plays a necessary role in rapid error prediction in humans. *Journal of Neuroscience*, *28*(51), 14000-14005.

Mostofsky, S. H., & Simmonds, D. J. (2008). Response inhibition and response selection: two sides of the same coin. *Journal of cognitive neuroscience*, *20*(5), 751-761.

Nambu, A., Tokuno, H., & Takada, M. (2002). Functional significance of the cortico–subthalamo–pallidal 'hyperdirect'pathway. *Neuroscience research*, *43*(2), 111-117.

Nasreddine, Z. S., Phillips, N. A., Bédirian, V., Charbonneau, S., Whitehead, V., Collin, I., ... & Chertkow, H. (2005). The Montreal Cognitive Assessment, MoCA: a brief screening tool for mild cognitive impairment. *Journal of the American Geriatrics Society*, *53*(4), 695-699.

Obeso, I., Cho, S. S., Antonelli, F., Houle, S., Jahanshahi, M., Ko, J. H., & Strafella, A. P. (2013). Stimulation of the pre-SMA influences cerebral blood flow in frontal areas involved with inhibitory control of action. *Brain Stimulation*, *6*(5), 769-776.

Obeso, I., Robles, N., Muñoz-Marrón, E., & Redolar-Ripoll, D. (2013). Dissociating the role of the pre-SMA in response inhibition and switching: a combined online and offline TMS approach. *Frontiers in human neuroscience*, *7*, 150.

Picton, T. W., Stuss, D. T., Alexander, M. P., Shallice, T., Binns, M. A., & Gillingham, S. (2007). Effects of focal frontal lesions on response inhibition. *Cerebral cortex*, *17*(4), 826-838.

Rae, C. L., Hughes, L. E., Weaver, C., Anderson, M. C., & Rowe, J. B. (2014). Selection and stopping in voluntary action: a meta-analysis and combined fMRI study. *Neuroimage*, *86*, 381-391.

Rieger, M., Gauggel, S., & Burmeister, K. (2003). Inhibition of ongoing responses following frontal, nonfrontal, and basal ganglia lesions. *Neuropsychology*, *17*(2), 272-282.

Roberts, R. E., & Husain, M. (2015). A dissociation between stopping and switching actions following a lesion of the pre-supplementary motor area. *Cortex*, *63*, 184-195.

Rorden, C., & Brett, M. (2000). Stereotaxic display of brain lesions. *Behavioural neurology*, *12*(4), 191-200.

Rorden, C., Karnath, H. O., & Bonilha, L. (2007). Improving lesion-symptom mapping. *Journal of cognitive neuroscience*, *19*(7), 1081-1088.

Simmonds, D. J., Pekar, J. J., & Mostofsky, S. H. (2008). Meta-analysis of Go/No-go tasks demonstrating that fMRI activation associated with response inhibition is task-dependent. *Neuropsychologia*, *46*(1), 224-232.

Smith, J. L., Mattick, R. P., Jamadar, S. D., & Iredale, J. M. (2014). Deficits in behavioural inhibition in substance abuse and addiction: a meta-analysis. *Drug and alcohol dependence*, *145*, 1-33.

Sperber, C., & Karnath, H. O. (2017). Impact of correction factors in human brain lesion-behavior inference. *Human Brain Mapping*, *38*(3), 1692-1701.

Stuss, D. T., & Alexander, M. P. (2007). Is there a dysexecutive syndrome?. *Philosophical Transactions of the Royal Society B: Biological Sciences*, *362*(1481), 901-915.

Swick, D., Ashley, V., & Turken, U. (2008). Left inferior frontal gyrus is critical for response inhibition. *BMC neuroscience*, *9*(1), 102.

Swick, D., Ashley, V., & Turken, U. (2011). Are the neural correlates of stopping and not going identical? Quantitative meta-analysis of two response inhibition tasks. *Neuroimage*, *56*(3), 1655-1665.

Tsuchida, A., & Fellows, L. K. (2009). Lesion evidence that two distinct regions within prefrontal cortex are critical for n-back performance in humans. *Journal of Cognitive Neuroscience*, *21*(12), 2263-2275.

van den Wildenberg, W. P., Burle, B., Vidal, F., van der Molen, M. W., Ridderinkhof, K. R., & Hasbroucq, T. (2010). Mechanisms and dynamics of cortical motor inhibition in the stop-signal paradigm: a TMS study. *Journal of cognitive neuroscience*, *22*(2), 225-239.

Verbruggen, F., Aron, A. R., Band, G. P., Beste, C., Bissett, P. G., Brockett, A. T., ... & Colzato, L. S. (2019). A consensus guide to capturing the ability to inhibit actions and impulsive behaviors in the stop-signal task. *Elife*, *8*, e46323.

Verbruggen, F., Aron, A. R., Stevens, M. A., & Chambers, C. D. (2010). Theta burst stimulation dissociates attention and action updating in human inferior frontal cortex. *Proceedings of the National Academy of Sciences*, *107*(31), 13966-13971.

Verbruggen, F., Chambers, C. D., & Logan, G. D. (2013). Fictitious inhibitory differences: how skewness and slowing distort the estimation of stopping latencies. *Psychological science*, *24*(3), 352-362.

Wiesen, D., Sperber, C., Yourganov, G., Rorden, C., & Karnath, H. O. (2019). Using machine learning-based lesion behavior mapping to identify anatomical networks of cognitive dysfunction: spatial neglect and attention. *NeuroImage*, *201*, 116000.

Zhang, R., Geng, X., & Lee, T. M. (2017). Large-scale functional neural network correlates of response inhibition: an fMRI meta-analysis. *Brain Structure and Function*, *222*(9), 3973-3990.

Zhang, Y., Kimberg, D. Y., Coslett, H. B., Schwartz, M. F., & Wang, Z. (2014). Multivariate lesion-symptom mapping using support vector regression. *Human brain mapping*, *35*(12), 5861-5876.

Table 1.

Demographic, clinical, and neuropsychological characteristics of healthy control and frontal patient groups.

	Healthy Controls	Frontal Patients					
		Dorsomedial	Ventromedial	Left Lateral	Right Lateral		
	Mean (*SD*)	Mean (*SD*)	Mean (*SD*)	Mean (*SD*)	Mean (*SD*)	F/χ^2	*p*
N	60	13	11	6	12	-	-
Age (yr)	52.8 (15.9)	57.9 (10.9)	52.5 (12.9)	48.5 (9.6)	50.0 (12.8)	1.10	.36
Sex (M:F)	26:34	6:7	3:8	3:3	1:11	7.56	.11
Education (yr)	15.0 (3.0)	13.9 (3.7)	14.3 (3.5)	14.5 (1.9)	12.6 (4.1)	1.55	.19
BDI	4.9 (4.6)	13.2# (12.5)	13.6# (6.9)	7.7 (8.4)	16.3# (9.3)	10.42	< .001***
ANART IQ^	123.2 (6.8)	121.2 (6.5)	121.3 (11.6)	112.5# (7.0)	113.3# (10.8)	5.16	< .001***
Backward digit span	5.2 (1.5)	5.2 (1.8)	4.3 (1.6)	3.5 (0.6)	4.5 (0.9)	2.82	.029*
Backward Corsi span	4.9 (1.2)	3.8 (1.5)	3.9 (1.6)	4.5 (0.6)	4.3 (1.1)	2.73	.033*
Fluency—F	14.4 (4.4)	9.4# (5.4)	13.9 (3.3)	6.3# (3.5)	11.2 (4.3)	7.87	< .001***
Fluency—Animal	21.7 (5.3)	17.8# (4.7)	18.7 (4.9)	12.3# (5.3)	15.6# (4.9)	7.83	< .001***
Sentence comprehension accuracy (%)	97.9 (6.2)	97.3 (5.5)	99.3 (2.4)	91.7 (7.6)	95.8 (7.7)	1.90	.12
Two-back d'_L	6.7 (1.8)	5.2 (1.5)	5.7 (2.6)	5.6 (2.0)	6.5 (2.2)	-	-
Two-back hit RT (ms)	695.5 (157.1)	807.9 (134.8)	664.4 (111.1)	815.6 (140.4)	742.4 (162.9)	-	-
Lesion volume (cc)	-	50.8 (60.8)	17.1 (13.3)	27.6 (15.6)	40.4 (24.8)	1.74	.18
Time after injury (yr)	-	4.0 (2.7)	4.1 (2.7)	4.0 (3.3)	4.7 (3.6)	0.14	.94

Note. ANART = American National Adult Reading Test; BDI = Beck Depression Inventory, MoCA = Montreal Cognitive Assessment. Sex distribution was compared using the Likelihood Ratio test. Asterisks indicate the significance level of ANOVA. *$p < .05$, ***$p < .001$. #Patients versus Healthy Controls (Tukey test: $p < .05$). ^Not all patients completed the ANART.

Table 2.

Stop-signal task performance of healthy control and frontal patient groups.

	Healthy Controls	Frontal Patients					
		Dorsomedial	Ventromedial	Left Lateral	Right Lateral		
	Mean (*SD*)	Mean (*SD*)	Mean (*SD*)	Mean (*SD*)	Mean (*SD*)	χ^2	*p*
N	60	13	11	6	12	-	-
Raw scores							
Mean go RT (ms)	613.9 (135.9)	714.7 (106.4)	620.0 (145.7)	742.2 (137.9)	788.8 (289.8)	-	-
Go accuracy (%)	98.7 (1.5)	98.6 (1.0)	96.9 (4.2)	98.2 (2.6)	98.7 (1.3)	-	-
Unsuccessful stop RT (ms)	509.7 (93.4)	599.1 (96.3)	501.1 (90.4)	589.6 (84.7)	597.4 (81.6)	-	-
Suppression rate (%)	56.8 (7.4)	57.4 (5.3)	53.6 (8.9)	61.0 (7.8)	59.5 (8.6)	-	-
Mean SSD (ms)	338.6 (96.0)	356.5 (64.4)	299.3 (117.4)	368.1 (65.4)	380.8 (90.6)	-	-
SSRT (ms)	278.9 (86.2)	346.7 (90.3)	313.0 (70.9)	379.9 (105.9)	427.5 (315.3)	-	-
***Z* scores**							
Mean go RT	0.00 (0.98)	0.68$^{\#}$ (0.92)	0.07 (1.16)	1.51$^{\#}$ (1.17)	1.20 (2.15)	14.57	.006**
Go accuracy	-0.16 (1.40)	-0.45 (1.12)	-1.80 (3.22)	-0.48 (2.20)	-0.55 (1.57)	5.79	.22
Unsuccessful stop RT	0.01 (0.98)	0.84$^{\#}$ (0.88)	-0.13 (0.95)	1.39$^{\#}$ (1.06)	0.83$^{\#}$ (1.14)	17.33	.002**
Suppression rate	0.00 (0.97)	-0.10 (0.91)	-0.52 (1.48)	0.96 (1.30)	0.18 (1.58)	5.25	.26
Mean SSD	0.00 (0.95)	0.05 (0.90)	-0.52 (1.32)	0.61 (0.80)	0.29 (1.26)	5.17	.27
SSRT	0.00 (1.03)	0.70 (1.13)	0.55 (0.97)	1.70$^{\#}$ (1.26)	1.61 (3.47)	14.22	.007**

Note. SSD = stop signal delay; SSRT = stop signal reaction time. Asterisks indicate the significance level of Kruskal–Wallis Tests. **$p < .01$. $^{\#}$Patients versus Healthy Controls (one-tailed Mann–Whitney *U* tests: $p < .013$; Bonferroni-corrected).

Figure Captions

Figure 1. Flow diagram of participant recruitment and progression through the study. HC = healthy controls; DM = dorsomedial; VM = ventromedial; LL = left lateral; RL = right lateral.

Figure 2. Representative axial slices and midsagittal views of the MNI brain, showing the degree of lesion overlap for subjects with damage affecting the dorsomedial (DM; top row), ventromedial (VM; second row), left lateral (LL; third row), and right lateral (RL; bottom row) frontal cortex. Colors indicate the degree of overlap across subjects, as shown in the legend.

Figure 3. Coronal slices (MNI coordinates = 8, 12, 16, and 18) of prefrontal regions that are consistently activated during successful stopping in the stop-signal task (Zhang et al., 2017) and damaged in our sample groups. The meta-analysis figure was reused under the terms of the Creative Commons Attribution 4.0 International License.

Figure 4. Boxplots of stop-signal reaction time (SSRT) in healthy controls (HC) and dorsomedial (DM), ventromedial (VM), left lateral (LL), and right lateral (RL) frontal patients. Asterisks indicate the significance level of Mann–Whitney *U* tests (patients versus HC). *$p < .05$, **$p < .013$

Figure 5. The power (top row) and statistical maps (second to bottom rows) of voxel-based lesion symptom mapping computed for stop-signal reaction time (SSRT; $n = 42$). Clusters of at least 50 significant voxels (red) are embedded in yellow circles (one-tailed Brunner–Munzel tests, thresholded at $p < .05$, uncorrected).

Figure 6. Boxplots of mean reaction time (RT) in (a) go trials and (b) failed stop-signal trials in healthy controls (HC) and dorsomedial (DM), ventromedial (VM), left lateral (LL), and right

lateral (RL) frontal patients. Asterisks indicate the significance level of Mann–Whitney *U* tests (patients versus HC). *$p < .05$, **$p < .013$

Figure 1.

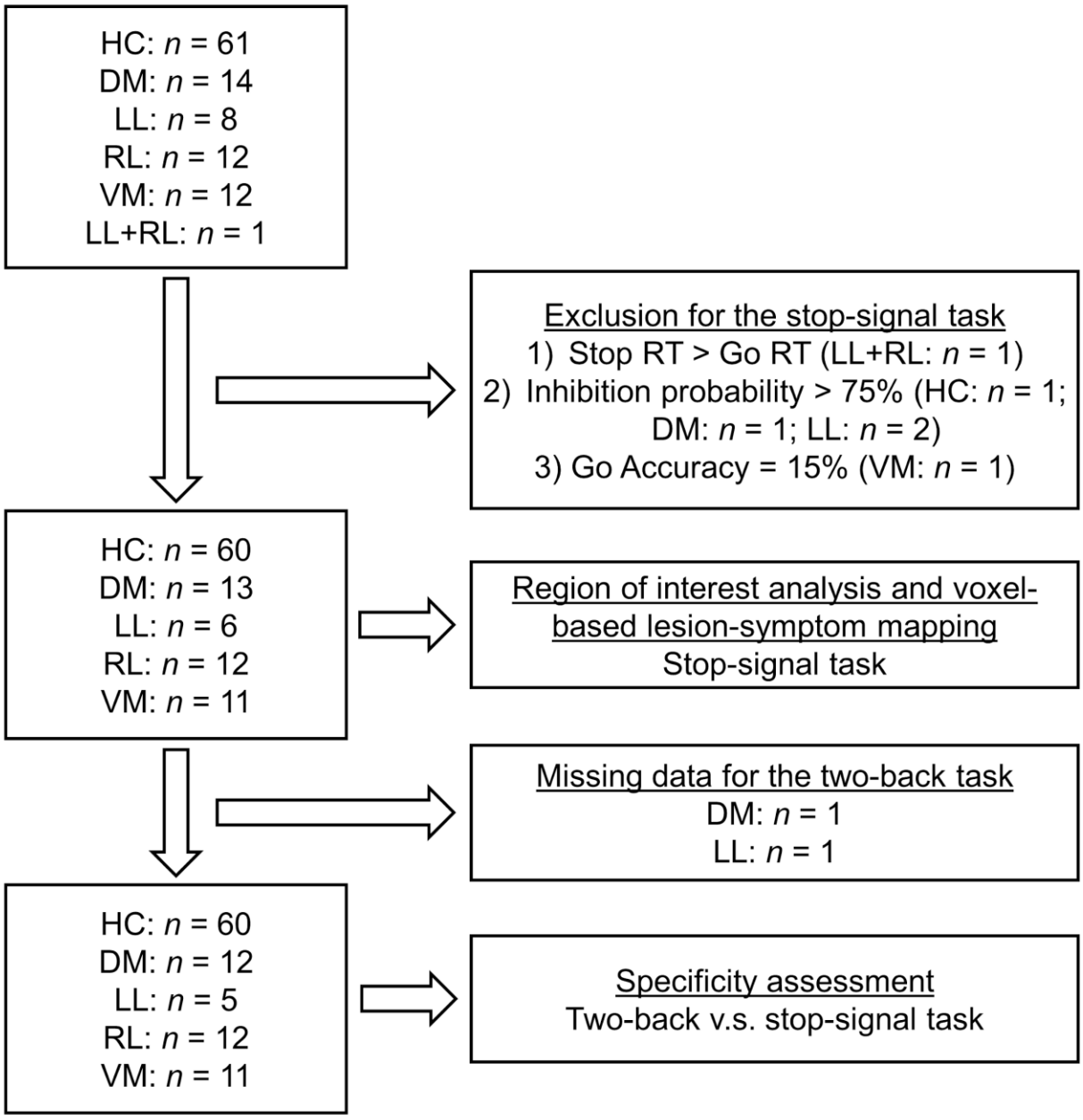
HC: n = 61
DM: n = 14
LL: n = 8
RL: n = 12
VM: n = 12
LL+RL: n = 1
Exclusion for the stop-signal task
1) Stop RT > Go RT (LL+RL: n = 1)
2) Inhibition probability > 75% (HC: n = 1; DM: n = 1; LL: n = 2)
3) Go Accuracy = 15% (VM: n = 1)
HC: n = 60
DM: n = 13
LL: n = 6
RL: n = 12
VM: n = 11
Region of interest analysis and voxel-based lesion-symptom mapping
Stop-signal task
Missing data for the two-back task
DM: n = 1
LL: n = 1
HC: n = 60
DM: n = 12
LL: n = 5
RL: n = 12
VM: n = 11
Specificity assessment
Two-back v.s. stop-signal task

Figure 2.

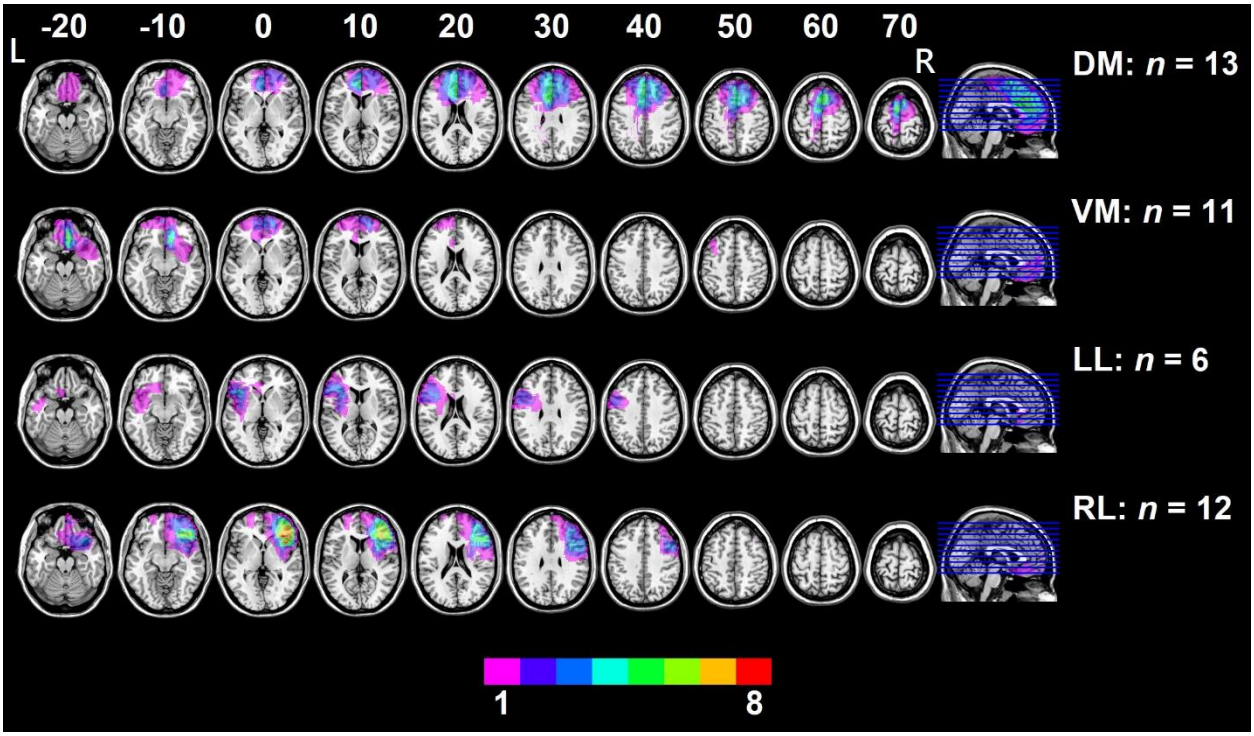

Figure 3.

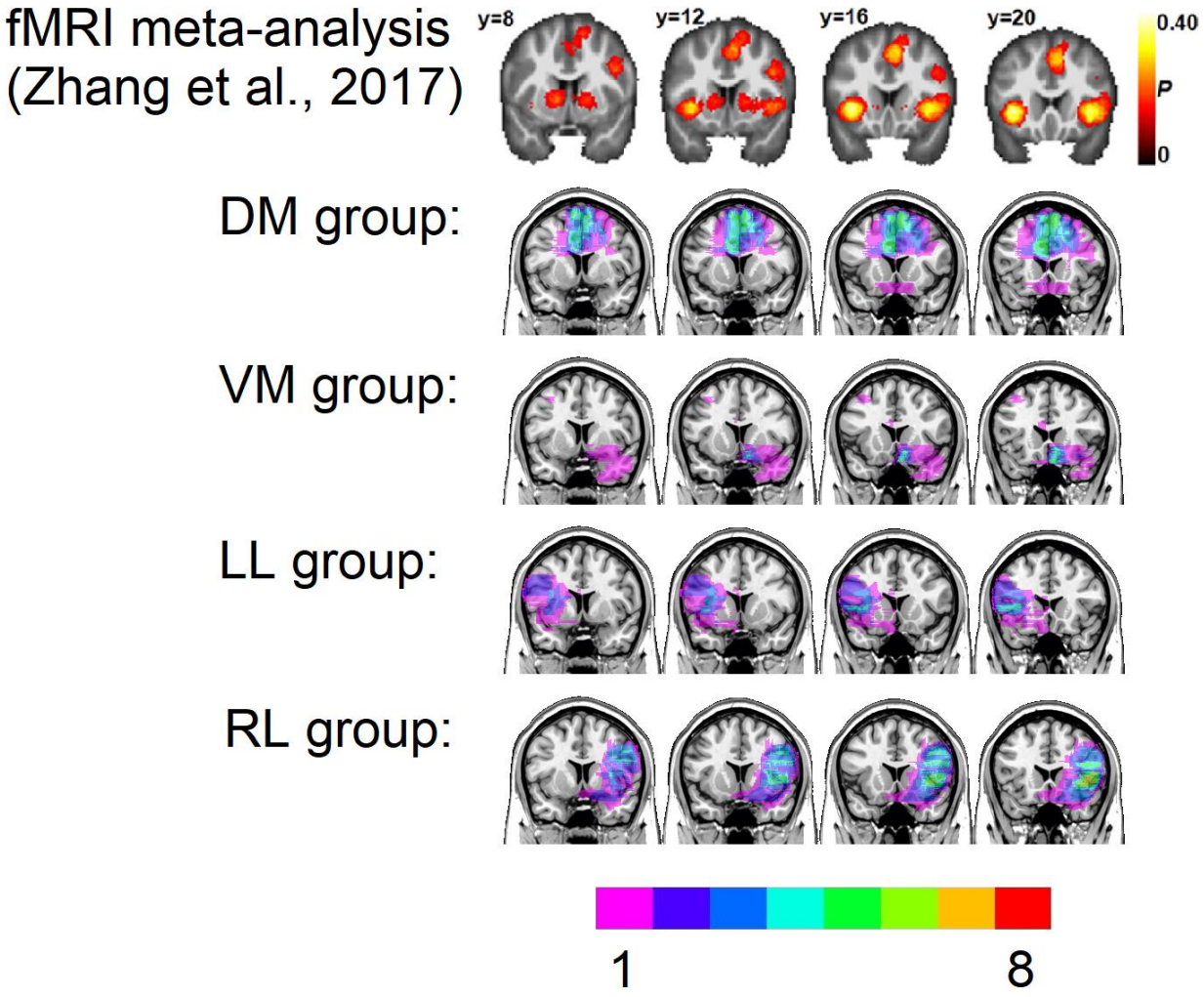
fMRI meta-analysis
(Zhang et al., 2017)
y=8
y=12
y=16
y=20
0.40
P
0
DM group:
VM group:
LL group:
RL group:
1
8

Figure 4.

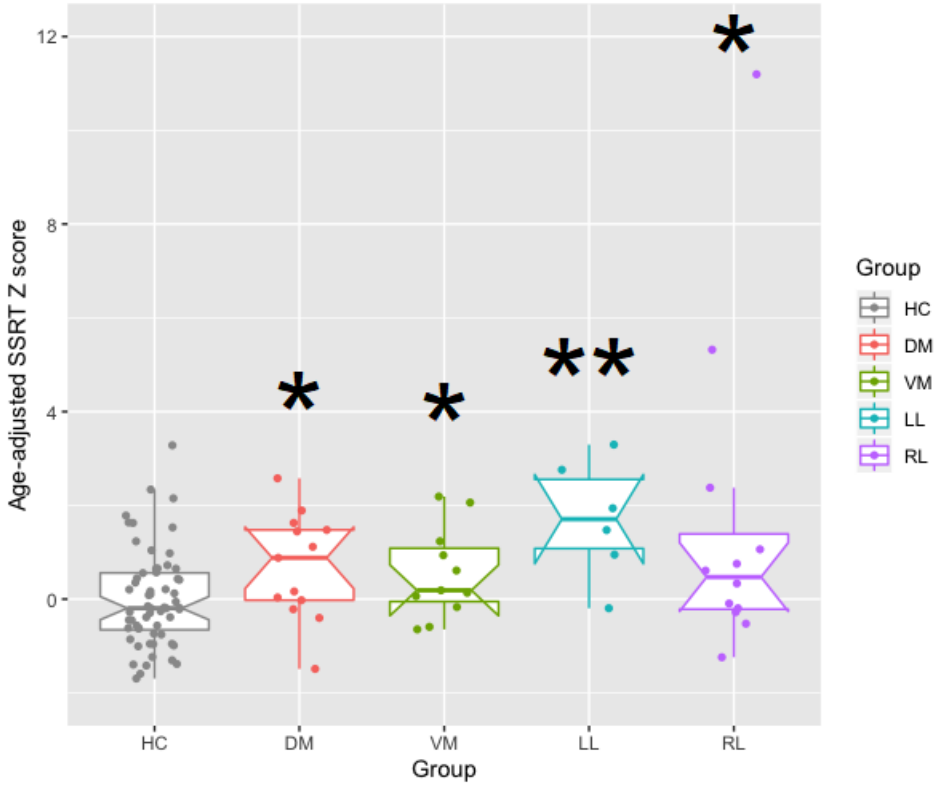
12
8
4
0
Age-adjusted SSRT Z score
*
*
**
*
HC
DM
VM
LL
RL
Group
Group
HC
DM
VM
LL
RL

Figure 5.

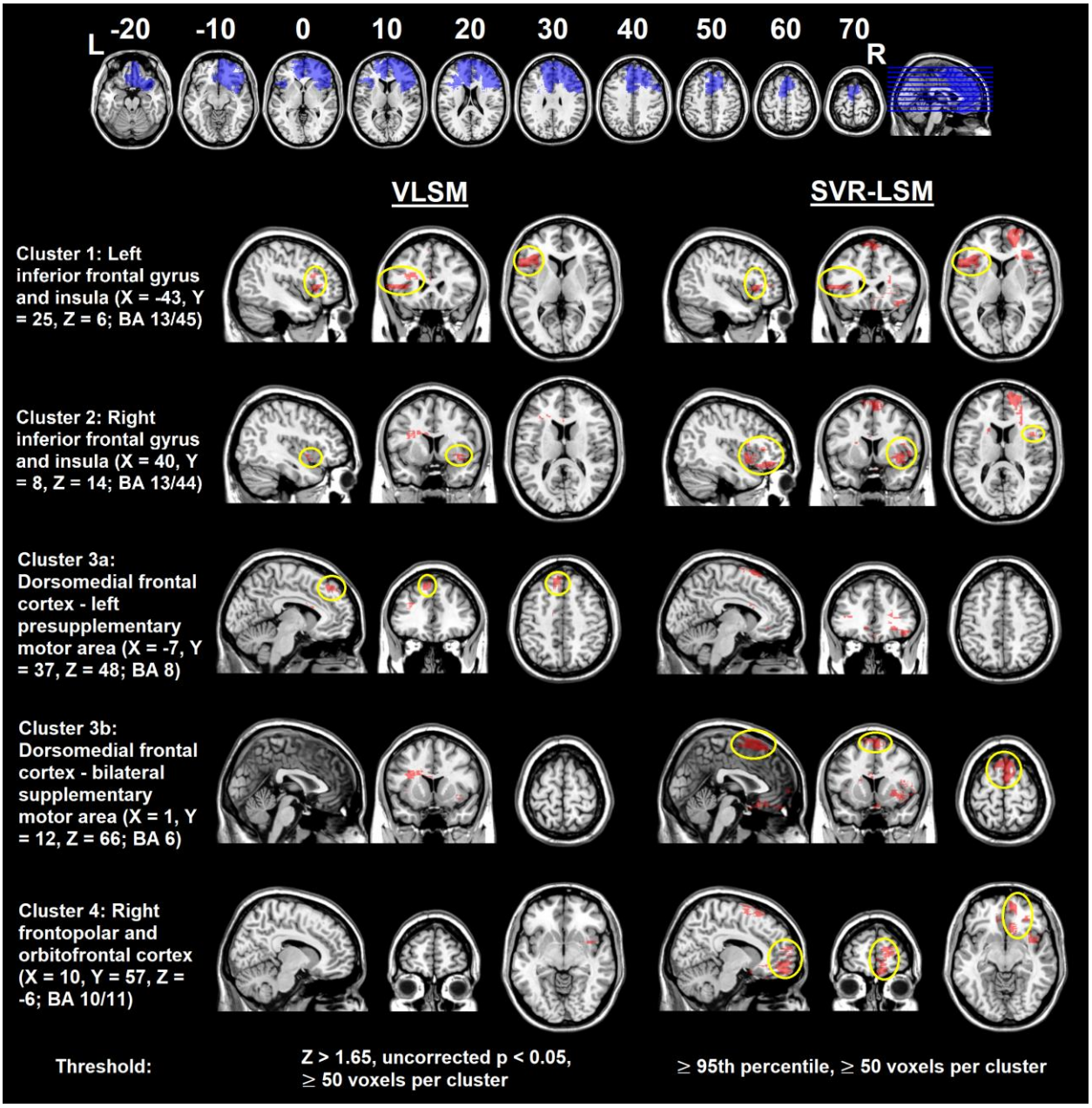
L
-20
-10
0
10
20
30
40
50
60
70
R
VLSM
SVR-LSM
Cluster 1: Left inferior frontal gyrus and insula (X = -43, Y = 25, Z = 6; BA 13/45)
Cluster 2: Right inferior frontal gyrus and insula (X = 40, Y = 8, Z = 14; BA 13/44)
Cluster 3a: Dorsomedial frontal cortex - left presupplementary motor area (X = -7, Y = 37, Z = 48; BA 8)
Cluster 3b: Dorsomedial frontal cortex - bilateral supplementary motor area (X = 1, Y = 12, Z = 66; BA 6)
Cluster 4: Right frontopolar and orbitofrontal cortex (X = 10, Y = 57, Z = -6; BA 10/11)
Threshold:
Z > 1.65, uncorrected p < 0.05, ≥ 50 voxels per cluster
≥ 95th percentile, ≥ 50 voxels per cluster

Figure 6.

(a)

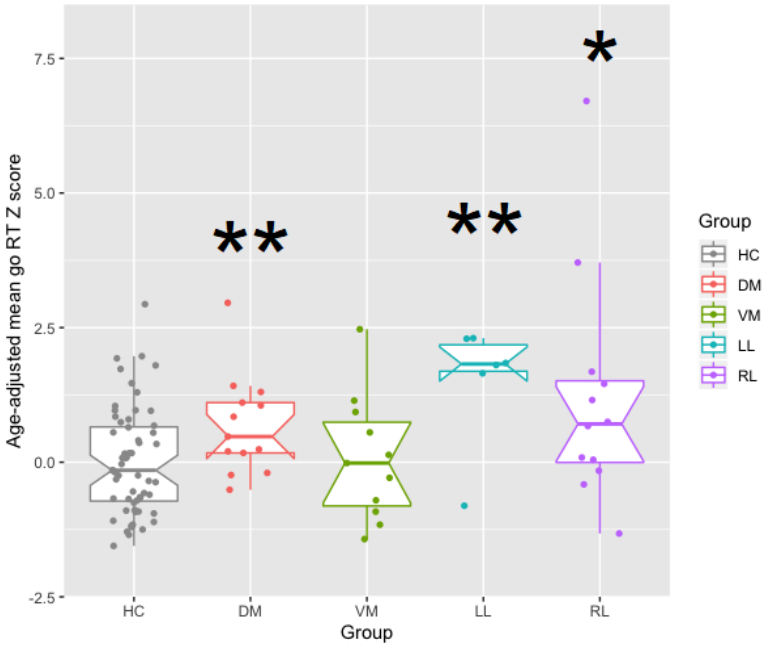
Age-adjusted mean go RT Z score
7.5
5.0
2.5
0.0
-2.5
HC
DM
VM
LL
RL
Group
*
**
**
Group
HC
DM
VM
LL
RL

(b)

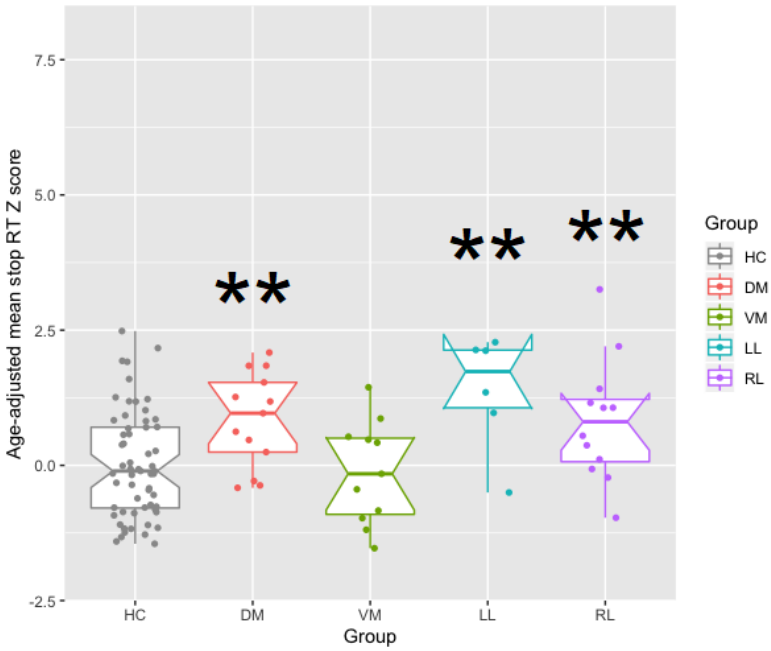
Age-adjusted mean stop RT Z score
7.5
5.0
2.5
0.0
-2.5
HC
DM
VM
LL
RL
Group
**
**
**
Group
HC
DM
VM
LL
RL